

# Structure and energetics of alkanethiol adsorption on the Au(111) surface

Yashar Yourdshahyan<sup>a)</sup> and Andrew M. Rappe

*Department of Chemistry and Laboratory for Research on the Structure of Matter,  
University of Pennsylvania, Philadelphia, Pennsylvania 19104-6323*

(Received 12 February 2002; accepted 12 April 2002)

The interaction of thiol molecules with the Au(111) surface was investigated with state-of-the-art first-principles methods. We report theoretical evidence for the existence of a physisorption precursor to chemisorption, in agreement with experiment. The origins of inconsistency in recent studies regarding the adsorption site, geometry, and energetics of CH<sub>3</sub>S on the Au(111) surface were also investigated. We show that the chemisorption site is between the hollow and bridge sites, with a large molecular tilting angle relative to the surface normal. The molecular structure of the overlayer is coverage dependent, with the molecular tilting angle increasing with decreasing coverage. Increasing chain length up to three carbon atoms affects both the chemisorption energetics and the tilt angle. The inconsistency of tilting angles, reported for the fcc site is found to be a consequence of multiple local minima. The ordered structure of thiol molecules at different coverages was also investigated, confirming the recent experimental findings that the  $c(4\times 2)$  structure model is preferred over  $(\sqrt{3}\times\sqrt{3})R30^\circ$ . © 2002 American Institute of Physics.  
[DOI: 10.1063/1.1483072]

## I. INTRODUCTION

Self-assembled monolayers (SAMs) have become a subject of intense interest in material science, because they provide stable and ordered structures on surfaces, with properties that are useful for a broad range of industrial applications, including protective coatings, wetting control, friction and lubrication control, adhesion, surface chemistry, optics, and electronics.<sup>1–3</sup> In particular, the adsorption process of *n*-alkanethiol molecules on gold surfaces has been given special attention. The relative simplicity of the molecules, the highly stable and ordered SAM structures, and the ease of preparation of the gold (111) surface make this system ideal for study with a variety of techniques. Both fundamental interest in the surface chemistry of SAMs and their technological significance motivate this work.

Despite the apparent simplicity of this system, the adsorption and growth of SAM structures of *n*-alkanethiolates, CH<sub>3</sub>(CH<sub>2</sub>)<sub>*n*</sub>S [Fig. 1(a)], on the Au(111) surface have been shown to be very complex, with many controversial results in both theoretical and experimental investigations. The overall process can be summarized as follows: (i) The sticking coefficient for alkanethiols on Au(111) is near unity at low temperature, and decreases with increasing temperature [starting when surface temperature (*T<sub>s</sub>*) is ~50 K below the desorption temperature].<sup>4</sup> (ii) The initial stage of adsorption is reported to start with a physisorbed state, with the molecules lying almost parallel to the surface [Fig. 1(b)].<sup>1</sup> (iii) Following the physisorption, alkanethiolates are dissociatively chemisorbed to the gold surface via the sulfur atom after cleavage of the S–H bonds [Fig. 1(b)]. (iv) In the low coverage regime or “lying-down” phase, the molecular axis of the chemisorbed molecules has been reported to be paral-

lel to the surface [Fig. 1(c)],  $\theta=90^\circ$ , with the C–C bonds stretched along the molecular axis.<sup>1</sup> (v) Increased coverage results in formation of ordered structures, where the hydrocarbon chains have a smaller tilt angle. Different structural phases are observed as coverage increases. (vi) At full coverage [we define full coverage ( $\Theta=1$ ) to mean saturation coverage, one thiol molecule per three gold surface atoms], the SAM structure is highly ordered, with two different structural models proposed: the hexagonal  $(\sqrt{3}\times\sqrt{3})R30^\circ$  lattice of alkanethiolates<sup>5,6</sup> [Fig. 1(e)], and the  $c(4\times 2)$  superlattice of the hexagonal one [Figs. 1(f) and 1(g)].<sup>7–10</sup> In the single chain hexagonal model, the S atom of each molecule is in a hollow site, with a tilt angle  $\theta\sim 32^\circ$ , and S–S spacing of ~5 Å. The  $c(4\times 2)$  model contains four molecules with two inequivalent chains per unit cell (different adsorption site, S–S spacing of ~2.2 Å, and different twist angle). For a more detailed review, interested readers are referred to Refs. 1 and 2. Several steps of this process contain fundamental unresolved issues that require investigation.

To illuminate SAM formation, several theoretical studies have provided information about the structure and energetics of thiol adsorption on the Au(111) surface. The earliest studies were based on highly simplified models (using small clusters or very thin slabs to represent the surface and ignoring structural relaxation) and have been unsuccessful in predicting the structural properties and energetics of this system. One example is the proposal of the hcp-hollow site as the favored adsorption position<sup>11,12</sup> which has been shown to be incorrect.<sup>13,14</sup> On the other hand, recent investigations<sup>13–19</sup> using density functional theory<sup>20</sup> based first-principles methods have been more successful.

Grönbeck *et al.* concluded that the dissociation of disulfide is favored and found evidence of a very strong S–Au bond at the fcc-hollow site with  $\theta=0^\circ$  (angle between S–C bond and surface normal, see Fig. 1) for the CH<sub>3</sub>S

<sup>a)</sup>Electronic mail: yashar@sas.upenn.edu

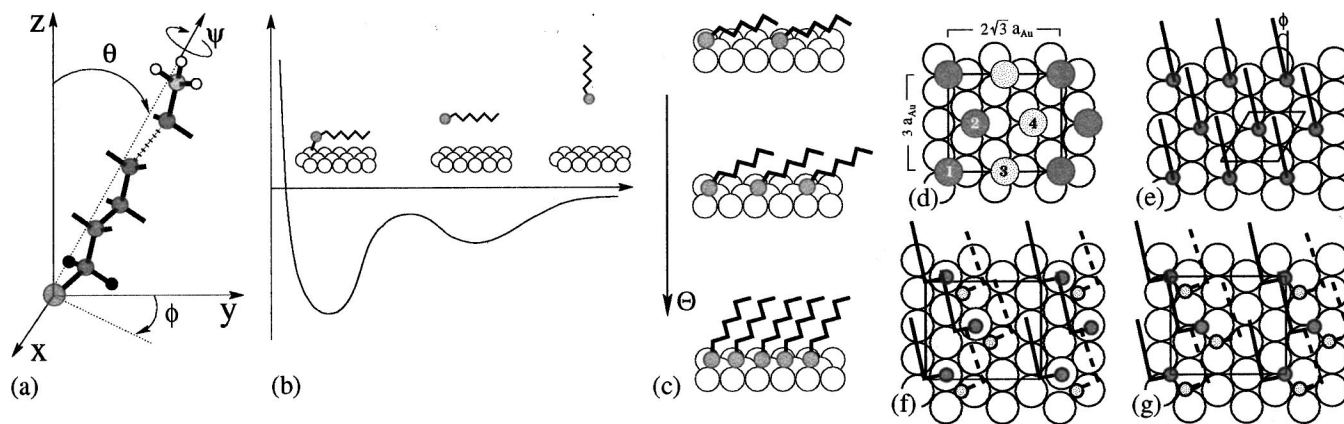


FIG. 1. The following are illustrated: (a) *n*-alkanethiol molecule (b) interaction potential between thiol molecule and Au(111) surface, (c) decreasing tilt angle,  $\theta$ , with increasing coverage,  $\Theta$ , (d) the symmetry of the  $c(4 \times 2)$  model, where molecules 1 and 2 are equivalent but distinct from 3 and 4, (e) hexagonal ( $\sqrt{3} \times \sqrt{3}$ ) $R30^\circ$  structure model, and (f) and (g) two different structural model for the  $c(4 \times 2)$  superlattice.

molecule.<sup>13</sup> Our recent study of the effect of coverage and chain length on thiolate adsorption (restricted to tilt angles near  $0^\circ$ ) pointed to the fcc-hollow site as the most stable position, independent of coverage and chain length.<sup>14</sup> A recently published study by Hayashi *et al.* investigated  $\text{CH}_3\text{S}$  adsorption at low and high coverage. Their results show the stable ground-state configuration of methylthiolate at full coverage to be a strongly tilted S–C bond at the bri-fcc site (shifted from the bridge site toward the fcc site) with a tilt angle of  $\theta = 52.7^\circ$  and adsorption energy  $E_{\text{ad}} = 0.54$  eV with respect to the free dimethyl-disulfide. The study by Akinaga *et al.* examined adsorption of thiol molecules on different metal surfaces, also reporting the bri-fcc site as the favored adsorption position in the case of Au(111),<sup>16</sup> with  $\theta = 51.94^\circ$  and  $E_{\text{ad}} = 1.84$  eV with respect to free  $\text{CH}_3\text{S}$ . The study performed by Vargas *et al.* proposed the bridge site as the stable site for adsorption regardless of coverage (very weak  $\Theta$  dependency was reported). They also reported that the adsorption energy of the thiol molecule at fcc site changes from  $\sim 0.78$  to  $\sim 0.13$  eV for  $\Theta$  of 0.25 to 1, respectively. The presented reason was different surface relaxation at different  $\Theta$ .<sup>17</sup> Finally, the study performed by Gottschalk *et al.*<sup>19</sup> at  $\Theta = 0.75$  reported the bri-fcc site for adsorption ( $\theta = 61.1^\circ$  and  $E_{\text{ad}} = 1.72$  eV with respect to free  $\text{CH}_3\text{S}$ ). The authors proposed steric repulsion between the Au and methyl group to be the reason for adsorption at the bridge site.

Even though the majority of recent studies point to bri-fcc site as the minimum energy adsorption site, there are still some disagreements, including the tilting angle of the S–C bond, coverage dependency, and the adsorption energy. The objective of this paper is to understand the thiol interaction with gold surface in the initial stages of the adsorption process and the ordered SAM structure at full coverage. This study is performed with state-of-the-art first-principles calculations, based on density-functional theory (DFT).<sup>20</sup> All of the first-principles calculations have been performed with the plane-wave pseudopotential code “DACAPO.”<sup>21</sup> The paper is organized as follows: Section II briefly presents the method and calculational details used throughout this investigation. In Sec. III, the results for adsorption of thiol on gold are

presented and discussed. In Sec. IV, conclusions and outlook are presented.

## II. COMPUTATIONAL DETAILS

The framework of the computational method used in this investigation is DFT,<sup>20</sup> using the code “DACAPO.”<sup>21</sup> Exchange and correlation (XC) are treated with the PBE form of the generalized gradient approximation (GGA).<sup>22</sup> The electron–ion interactions are described by ultrasoft pseudopotentials (USPPs).<sup>23</sup> New pseudopotentials, H ( $1s^1$ ), C ( $2s^2 2p^2$ ), S ( $3s^2 3p^{3.5} 3d^{0.5}$ ), and Au ( $5d^{9.5} 5s^1 6p^{0.5}$ ), were generated within the USPP scheme using the PBE XC functional<sup>22</sup> (including relativistic effects and core corrections) with cutoff radii ( $r_c$ ) of 0.60, 1.24, 1.45, and 2.00 bohr, respectively. The transferability error in all generated potentials is in the meV range.<sup>14</sup> The plane wave cutoff is taken to be 25 Ry, which provides good total energy convergence. The Brillouin zone is sampled according to the Monkhorst–Pack method.<sup>24</sup> To improve the  $k$ -point convergence, the Fermi discontinuity is smoothed using temperature broadening with an effective electron temperature of 0.1 eV.<sup>25</sup>

The choice of slab size (6 Au layer),  $k$  points (2–6), and cutoff energy (25–30 Ry) is based on our tests in previously published work, which show converged calculations with an error of about 0.01 eV.<sup>14</sup> To assess the reliability of our method, and in particular the quality of the generated pseudopotentials, extensive calculations for properties of bulk and surface Au, and energetics of thiol molecules ( $\text{RS-H}$  and  $\text{RS-SR}$ ,  $\text{R}=\text{CH}_3$ ) in the gas phase were carried out. The results are summarized in Table I.

The theoretical results show higher lattice constants, lower surface energies, and lower bulk moduli than experiment for gold. This is a well-known effect of the GGA. The accuracy of our pseudopotentials is confirmed by excellent agreement with all-electron results. Furthermore, all investigations have difficulty in reproducing the experimental values of binding energy for  $\text{RS-H}$  and  $\text{RS-SR}$  ( $\text{R}=\text{CH}_3$ ). This difficulty will certainly affect the quality of calculated

TABLE I. The bulk and surface parameters of gold and the energetics of thiol molecules. Lattice constant  $a$  (Å), bulk modulus,  $B$  (MPa), surface energy,  $\gamma$  (J/m<sup>2</sup>), cohesive energy,  $E_{\text{coh}}$  (eV), of gold, and binding energies:  $E_d(\text{RS-H})$  and  $E_d(\text{RS-SR})$  in (eV),  $\text{R}=\text{CH}_3$ . The theoretical results are based on plane wave pseudopotential (PWPP) or the full potential linearized augmented plane wave (FPLAPW) methods with either PBE, PW91, or RPBE XC functional.

Ref.	Method (functional)	$a$	$B$	$E_{\text{surf}}$	$E_{\text{coh}}$	$E_d(\text{RS-H})$	$E_d(\text{RS-SR})$
This work	PWPP (PBE)	4.156	140.9	0.820	3.20	3.88	2.95
13	PWPP (PW91)	4.150			3.15	3.95	3.12
15	PWPP (PW91)	4.150	137.0	0.720	3.06		2.77
17	PWPP (PW91)	4.138	146.5	0.758		3.99	3.04
19	PWPP (RPBE)	4.180				1.68	3.05
26	FPLAPW	4.160	142.0				
2, 27, 28	Expt.	4.058–4.080	172.0–173.2	1.045–1.500	3.81	3.73	2.81

adsorption energies. A comparison between LDA and GGA shows that LDA overbinds even more.<sup>13</sup> The alternative RPBE functional has shown many excellent results for binding energies. For this system, it is worth noting that the RPBE functional does not show promising results.<sup>19</sup>

### III. RESULTS AND DISCUSSION

Study of a long chain thiol molecule interacting with the gold surface is computationally challenging due to the complexity of the system. Therefore, we chose to investigate the interaction of short-chain thiol molecules (up to three carbon atoms) with the Au(111) surface. The calculations presented here focus on the initial stages of adsorption, and results are compared to the experimental and other theoretical studies.

The adsorption energies have been calculated as

$$E_{\text{ad}} = -(E_{\text{SAM}} - E_{\text{Au}} - E_{\text{mol}}),$$

where,  $E_{\text{SAM}}$ ,  $E_{\text{Au}}$ , and  $E_{\text{mol}}$  represent the total energy of the SAM system (adsorbant plus substrate), clean gold surface, and the adsorbant molecule in gas phase, respectively.

#### A. Search for physisorption state

It has been reported that at low surface temperature ( $T_s$ ) and coverage ( $\Theta$ ), the dominant pathway to chemisorption is through physisorption.<sup>1,4,29</sup> In this state, alkanethiol molecules become trapped in the physisorption well for a relatively long period. The effective barrier height toward chemisorption has been estimated to be  $\sim 0.3$  eV, independent of chain length (for  $n > 6$ ). The physisorption energies,  $E_{\text{phys}}$ , for methanethiol, ethanethiol, and decanethiol have been reported to be 0.50, 0.59, and 1.08 eV, respectively.<sup>4,29</sup> Interpolating the presented values yields an estimated  $E_{\text{phys}}$  for  $\text{CH}_3\text{CH}_2\text{SH}$  of  $\sim 0.54$  eV.

Even though the van der Waals interaction, which is the major driving force for physisorption, is not included correctly in the current DFT functional, we attempt to study this initial stage to see if the physisorbed state could be distinguished. We performed a number of calculations using  $\text{CH}_3\text{SH}$ ,  $\text{CH}_3\text{CH}_2\text{SH}$ , and  $\text{CH}_3(\text{CH}_2)_2\text{SH}$  molecules adsorbed on the Au(111) surface (12 Au atoms per layer,  $\Theta = 0.25$ ). Molecules were placed with  $\theta = 0^\circ$  and  $90^\circ$ , at a distance,  $d_{\text{S-Surf}}$ , of 5, 3.5, and 2.8 Å to the surface, and then the hydrocarbon chain was relaxed.

We find that far from the surface, the thiol molecules prefer to stay in the stretched zigzag C–C–C line with molecular axis almost parallel to the surface (Fig. 2),  $\theta = 87^\circ$ , and adsorption energies of 0.07, 0.08, and 0.10 eV for each respective molecule. We also notice that the increase in C–C bond length is chain length dependent [ $\Delta d_{\text{C-C}} = 3\%$  and  $8\%$  for  $\text{CH}_3\text{CH}_2\text{SH}$  and  $\text{CH}_3(\text{CH}_2)_2\text{SH}$ , respectively]. As the distance decreases, the molecules start to relax, making a small angle with the surface. Noticeable is the trend of decreasing adsorption energy with shorter chains, which agrees with experimental results.

A careful search for the physisorption state of the  $\text{CH}_3\text{CH}_2\text{SH}$  molecule was carried out by calculating the total energy of the system with much smaller changes of  $d_{\text{S-Surf}}$ . The results show a physisorption state with an adsorption energy of 0.32 eV at 3.35 Å from the surface. The height of the calculated barrier toward chemisorption is 0.09 eV (Fig. 2). Unfortunately, these values are much smaller than the values estimated from experimental work. This is not surprising at all, due to incomplete description of van der Waals interaction in our method and the fact that the choice of molecular orientation and the adsorption site will affect the calculated barrier. Unfortunately, it is very hard to identify the true reaction coordinate at this state of adsorption mechanism due to the complex nature of the system. However, it is gratifying to find qualitative agreement with ex-

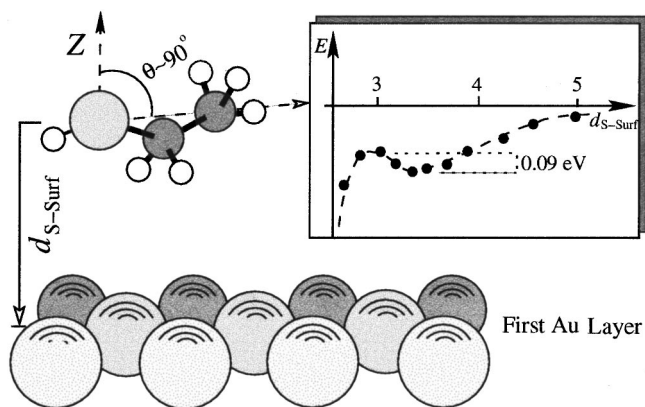


FIG. 2. Schematic picture of structural orientation for physisorbed state. The molecule is positioned over the fcc site, almost parallel to the surface with distance  $d_{\text{S-Surf}} = 3.35$  Å, from the surface plane.



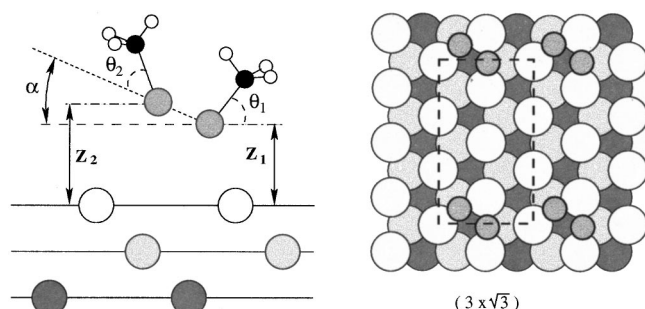


FIG. 3. Schematic picture of a DMDS molecule adsorbed on a Au(111) surface. ( $Z_1, \theta_1$ ) and ( $Z_2, \theta_2$ ) are distances from the surface plane and molecular angles with the surface normal for each S atom.

periment, and quantifying the magnitude of DFT error is a useful benchmark for future work in this era.

## B. Energetics and structure of thiolate adsorption

The next step of the adsorption process is dissociation and chemisorption. To investigate these states, the interaction of  $(\text{CH}_3\text{S})_2$ ,  $\text{CH}_3\text{S}$ ,  $\text{CH}_3\text{CH}_2\text{S}$ , and  $\text{CH}_3(\text{CH}_2)_2\text{S}$  molecules with Au(111) surface have been studied. Even though these molecules are the smallest thiol molecules, they do present a variety of difficulties when investigated theoretically. A free alkanethiolate molecule prefers a zigzag C–C–C conformation with a twist angle ( $\psi$ ) around the molecular axis, which varies with the chain length. When a metal surface is exposed to this molecule, the head group (S) location and the two angular dependencies,  $\theta$  and  $\phi$  [Fig. 1(a)], will play an important role in adsorption energetics.

### 1. Adsorption of dimethyl disulfide

Experimental and recent theoretical studies have characterized a dissociative process for dimethyl disulfide (DMDS),  $(\text{CH}_3\text{S})_2$ , when adsorbed on the Au(111) surface at low coverage. On the other hand, dimerization upon adsorption at high coverage is a proposed mechanism in ordered SAM structure, resulting in a  $c(4 \times 2)$  superlattice (see Sec. III C).

Our calculated structural parameters and dissociation energy of DMDS in the gas phase show very good agreement with both experimental data and other theoretical calculations (see Table II for details). The adsorption of DMDS on the Au(111) surface was investigated for  $\Theta = 1, 1/2$ , and  $1/3$ , using three different unit cells,  $(3 \times \sqrt{3})$ ,  $(3 \times 2\sqrt{3})$ , and

TABLE II. The structural parameters of dimethyl disulfide in the gas phase, compared to experiment and theory.  $d_{\text{S-S}}$  and  $d_{\text{S-C}}$  represent the equilibrium bond lengths of S–S (Å) and S–C (Å). The dissociation energy or bond strength,  $E_{\text{S-S}}$ , is given in eV. This work was performed with the PBE functional, and all other theoretical values were calculated using the PW91 functional.

Property	This work	Ref. 15	Ref. 13	Ref. 19	Expt.
$d_{\text{S-S}}$ (Å)	2.046	2.057			2.038 <sup>a</sup>
$d_{\text{S-C}}$ (Å)	1.817	1.822			1.810 <sup>a</sup>
$E_{\text{S-S}}$ (eV)	2.93	2.77	3.12	3.05	2.81 <sup>b</sup>

<sup>a</sup>Reference 27.

<sup>b</sup>Reference 28.

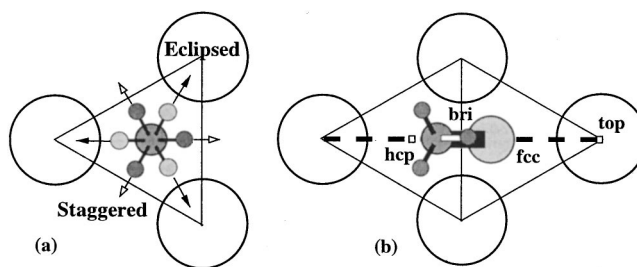


FIG. 4. Schematic picture for the orientation of a  $\text{CH}_3$  molecule adsorbed on the gold (111) surface, (a) the staggered and eclipsed orientations of H atoms, (b) structural orientation of the molecule. The thick dashed line shows our choice of diffusion path going through top, fcc, bri, and hcp sites.

$(3 \times 3\sqrt{3})$ , respectively. For  $\Theta = 1$  and  $1/2$  we find that DMDS is stable on the gold surface, see Fig. 3 and Table III for details. The results show that a single molecule adsorbed on the surface chemisorbs with S–S distance of 2.16–2.29 Å and  $E_{\text{ad}} \approx 0.2$ –0.3 eV depending on the coverage. Furthermore, the calculated induced charge density indicates that S–S head group binds to the surface through the nearest S atom, in agreement with experiment.

In the low coverage regime,  $\Theta = 1/3$ , the DMDS molecule dissociates and forms two methylthiolates on the surface (note that due to the large number of atoms needed for the calculations we used only four instead of six layers of Au in this slab geometry) in agreement with experimental findings. The calculated dissociation energy is 0.38 eV, which is in good agreement with other theoretical studies but is far from the experimental value of 1.04 eV.<sup>3</sup> The disagreement with experiment may be due to the difference between  $\Theta = 1/3$  and experimentally studied coverage.

### 2. Adsorption of methylthiolate

To examine the interaction of methylthiolate ( $\text{CH}_3\text{S}$ ) with gold, we first calculated total energies at full coverage. The molecule was adsorbed on different sites, using various S–C tilt angles relative to the surface normal, and different orientations of hydrogen atoms with respect to the surface gold atoms. Two high symmetry orientations for the hydrogen atoms were considered, staggered, and eclipsed. The calculated total energies indicate that independent of the head group position and tilt angle, the methyl hydrogen atoms prefer the staggered orientation, with C–H bonds pointing toward the bridge sites, [Fig. 4(a)]. We also find that the S–C bond prefers to point toward the bridge site [Fig. 4(b)].

Recent publications have reported a variety of tilting angles and  $d_{\text{S-Surf}}$  values for chemisorption at the fcc site. To

TABLE III. Energetic and structural parameters for single DMDS adsorbed on the Au(111) surface.  $E_{\text{ad}}$  is given with respect to free DMDS molecule.

Property	This work		Ref. 15	Ref. 17	
	1	1/2	1	1	1/2
$E_{\text{ad}}$ (eV)	0.198	0.276	0.169	0.191	0.255
$Z_1, Z_2$ (Å)	2.76, 3.20	2.60, 3.09	2.65, 2.97	2.86, —	2.84, —
$d_{\text{S-Au}}$ (Å)	2.85, 3.29	2.78, 3.04	2.69, 3.13	3.00, —	2.98, —
$d_{\text{S-S}}$ (Å)	2.16	2.29			

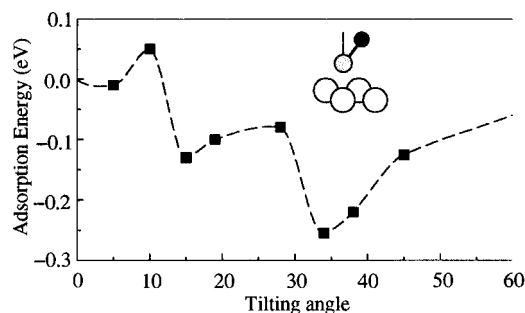


FIG. 5. Calculated total energy at full coverage with respect to S-C tilting angle ( $\theta$  [deg]), when methylthiolate is adsorbed on a fcc-hollow site.

investigate this, we calculated the total energies of methylthiolate on Au(111) using different starting tilt angles. The lateral positions of S and C were fixed to avoid lateral displacement. The hydrogen atoms were allowed to move freely, and the S and C were allowed to move in  $z$  direction ( $z$  direction is perpendicular to the surface). The calculated total energy values with respect to the angle, Fig. 5, show that there are a number of local minima for adsorption at the fcc site. This may explain the different angles found in the recent studies. Similar profiles with multiple local minimum angles are also found when the molecules are positioned at other high symmetry positions.

To further illuminate the multiple minima in this system, we calculated a two-dimensional potential energy surface (PES) (Fig. 6) along the diffusion path [Fig. 4(b)] for various tilt angles. To obtain the PES, total energies and forces are calculated with various  $\theta$  between 0 and  $60^\circ$  and various positions along the diffusion path. Note that the hydrogen atoms were fixed in the staggered orientation, and  $d_{S-Surf}$  and  $d_{S-C}$  were fixed at the average calculated values at each high

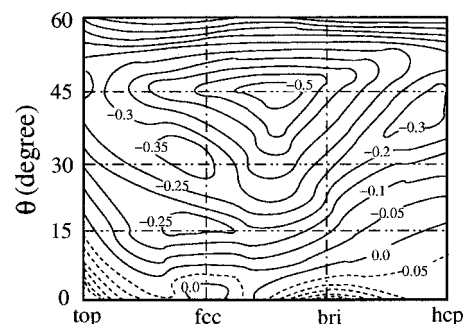


FIG. 6. Showing two-dimensional PES of thiol molecule on Au(111) surface. Energy values (eV) are given with respect to adsorption at the fcc site with  $\theta=0^\circ$ . The energy difference between the contours is 0.05 eV, with dashed lines representing positive values.

symmetry point found in the literature. For a smoother PES, a bicubic interpolation algorithm is used, taking into account forces of all atoms and energies at each point.<sup>30</sup> The PES results indicate that at full coverage the minimum adsorption energy is when the molecule has a tilt angle of  $\sim 45^\circ$  and it is positioned between bridge and fcc-hollow site. Furthermore, it shows clearly the existence of multiple local minima.

To complement the PES, full relaxations were performed. The methylthiolate molecule was adsorbed at each high symmetry position (top, fcc, bri, hcp) using the staggered orientation for hydrogen atoms and tilt angle of  $30^\circ$ . The systems were then fully relaxed (all atoms in the thiol molecule and two outermost Au layers are relaxed in  $x$ ,  $y$ , and  $z$  directions and the third Au layer only in the  $z$  direction) until a force-free situation was achieved, i.e., the sum of forces left in the structure was less than  $0.05 \text{ eV/\AA}$ .

The picture that emerges from our calculations is in agreement with the majority of the recent calculations. The

TABLE IV. Various parameters for adsorption of  $\text{CH}_3\text{S}$  on the Au(111) surface. Presented parameters are; the coverage,  $\Theta$ , adsorption energy,  $E_{\text{ads}}$  (eV), distance between S and surface layer (averaged position of surface atoms),  $d_{S-Surf}$  ( $\text{\AA}$ ), shortest Au-S bond length,  $d_{S-Au}$  ( $\text{\AA}$ ), the angle between the surface normal and S-C bond,  $\theta$  (deg), and the lateral displacement of S atom with respect to the ideal position,  $\delta$  ( $\text{\AA}$ ).

Site	Ref.	$\Theta$	$E_{\text{ads}}$	$d_{S-Au}$	$d_{S-surf}$	$\theta$	$\delta$
fcc	This work	1	1.49	2.59	1.92	34.4	
		0.5	1.45	2.56	1.89	39.5	
		13	1	2.39		0.00	
		15	1	1.42	2.52	1.78	16.7
		16	1	1.76	2.58	1.97	0.1
		17	1	1.45			
		19	0.75	1.49	2.66	2.04	55.7
bri-Fcc	This work	1	1.73	2.50	2.03	43.2	0.42
		0.5	1.69	2.49	2.04	50.3	0.49
		0.25	1.65	2.49	2.04	54.3	0.50
		15	1	1.66	2.50	2.05	52.7
		16	1	1.84	2.56	2.09	46.9
		17	1	1.79		2.09	58.0
		19	0.75	1.72	2.55	2.07	61.1
bri-Hcp	This work	1	1.65	2.53	2.08	51.3	0.28
		0.5	1.60	2.50	2.06	58.7	0.31
		15	1	1.63	2.50	2.09	53.4
		16	1	1.82	2.57	2.11	49.6
		19	0.75	1.70	2.55	2.07	61.0

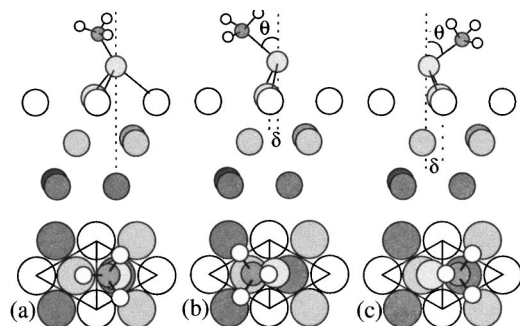


FIG. 7. Schematic picture of methylthiolate adsorbed on the Au(111) surface at (a) fcc, (b) bri-fcc, and (c) bri-hcp sites. Large circles represent Au atoms, where white is the top layer, light gray is the second layer, and dark gray is the third layer.

thiolate adsorbed on the Au(111) surface chemisorbs on bridge site with some distortion ( $\delta$ ) of the lateral S atom position toward the fcc site. Table IV summarizes our results for adsorption energies and structural parameters of the fully relaxed system as well as results from other investigations. Figures 7(a)–7(c), illustrate the structure of these adsorption sites, where Fig. 7(b) corresponds to the minimum energy position (bri-fcc). The calculated adsorption energy is in very good agreement with both theoretical and experimental values of 1.66–1.72 and 1.73 eV, respectively.<sup>2,15,19</sup> As can be seen from Table IV, the major disagreement is when the molecule is adsorbed on the fcc site. The origin for this is the existence of multiple local minima, as shown in Figs. 5 and 6. Figure 8 shows a cut through the Au–S bonds of the

induced charge densities for thiol at fcc and bri-fcc sites, with red as high induced charges. The bri-fcc case shows a larger concentration of electrons between Au and S, indicating stronger binding.

The question of *why thiolate molecules adsorbed on the Au(111) surface prefer the bridge site with lower coordination over the higher coordinated fcc site* still remains to be answered. Steric forces have been suggested as the origin for this behavior.<sup>18,19</sup> Our analysis of structural parameters ( $d_{S-Au}$ ,  $d_{S-surf}$ ,  $\theta$ , Au–S–C angle, and the surface atom positions) for methylthiolate adsorbed on high symmetry sites (fcc, fcc-bri, and top) indicates the existence of a preferred Au–S–C angle of about  $105^\circ$ – $115^\circ$ , in line with the findings of Krüger *et al.*<sup>18</sup> of  $105^\circ$ . As they pointed out, the existence of such angular preference, which is similar to C–C–S bond angle of  $108^\circ$ – $116^\circ$ , may indicate a distinct directionality for S–Au bonds at the surface. Furthermore, they show that positioning the thiol headgroup over the fcc site will result in larger Au–S–C angles for the unrelaxed surface. When the surface is relaxed, the  $d_{Au-Au}$  will become much larger than bulk values. Our calculations confirm a 10% increase in Au–Au distances and a large surface buckling when thiol molecules are adsorbed on fcc sites. Since there is no experimental evidence to support such large local reconstruction of the Au(111) surface, we believe that the existence of a preferred angle leads to the steric forces that move the molecule to lower coordinated absorption site in order to avoid this local reconstruction and minimize the energy. This issue should be addressed in more detail by analyzing the nature of thiol molecule bonding in different environments.

### 3. Coverage and chain length effect

To investigate the coverage dependency of thiol adsorption, additional total-energy calculations were performed for  $CH_3S$  adsorbed on a  $(2\sqrt{3} \times \sqrt{3})$  Au overlayer, i.e.,  $\Theta = 0.5$ .

Three high symmetry positions were considered and each system was fully relaxed. Calculations were also carried out for  $\Theta = 0.25$  with the molecule at the bri-fcc site. The results (Table IV) show that a decrease in the coverage results in an increase of tilt angle, in agreement with experimental data.

Next, the  $CH_3CH_2S$  molecule was adsorbed on a  $c(4 \times 2)$  Au overlayer, i.e.,  $\Theta = 0.25$ , Fig. 9(a). The molecule was positioned with the S atom 3 Å above the bridge site with a tilt angle of  $\theta = 50^\circ$ . Two different molecular orientations were chosen as the starting point,  $\theta > \theta_1$  and  $\theta < \theta_1$ , and the whole system was then fully relaxed. The fully optimized structure, Fig. 9(a), shows a molecular tilt angle of  $\theta = 58^\circ$  (molecular tilt angle),  $\theta_1 = 49^\circ$ , and  $\psi = 16^\circ$  with  $d_{S-surf} = 2.05$  Å, and adsorption energy of 1.76 eV. The calculated induced charge density (Fig. 9) indicates strong bonding in the thiol molecule (large electron density localization along the C–C and C–H bonds and localized electron density between C and S) and localized electron density between S and Au atoms at the bridge site indicating S–Au bonding.

Starting with the relaxed structure of  $CH_3CH_2S$ , an additional  $CH_2$  was inserted and the 3-carbon thiol then fully relaxed. The calculated values are  $\theta = 56^\circ$ ,  $\theta_1 = 53^\circ$ ,  $\theta_2$

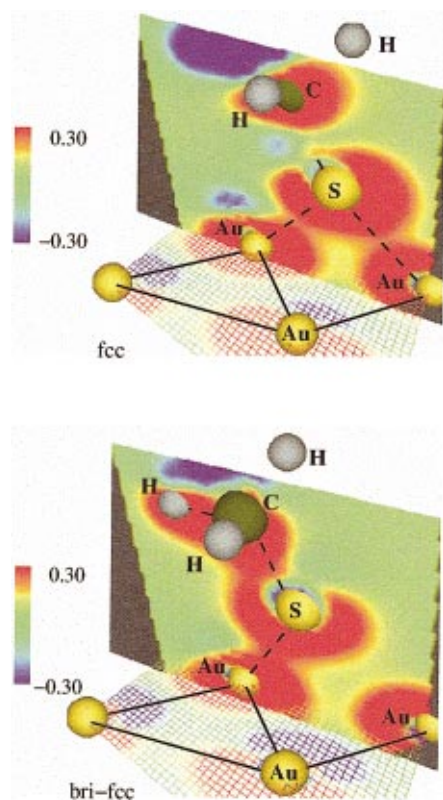


FIG. 8. (Color) The induced charge density for methyl thiolate molecule adsorbed at fcc (top figure) and bri-fcc site of the Au(111) surface.



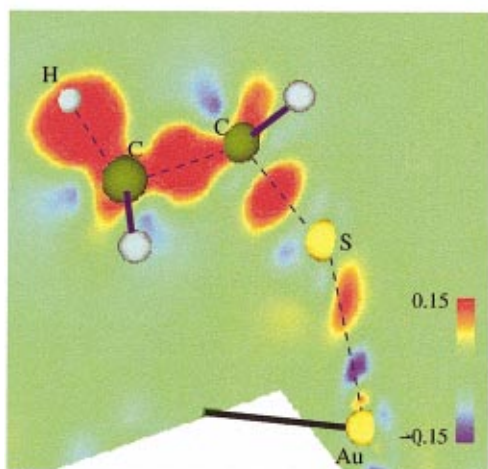
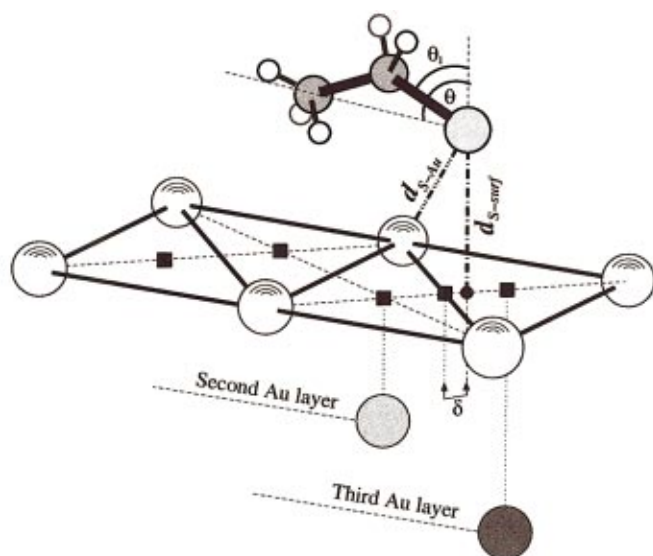


FIG. 9. (Color) Schematic picture of structural details (left) and calculated induced charge density (right) of an ethanethiolate molecule adsorbed on the gold (111) surface. The following labeling is used; the distance between S and surface,  $d_{S-surf}$ , the distance between S and nearest Au atom,  $d_{S-Au}$ . The angle between S-C and the surface normal,  $\theta_1$ , molecular tilt angle,  $\theta$ , and the distortion from the bridge site,  $\delta$ . Note that the induced charge density plot shows two planes, through C-C-S and S-Au-Au.

$=46^\circ$ , and  $\psi=21^\circ$  with  $d_{S-surf}=2.06$  Å, and adsorption energy of 1.81 eV. The results show very small changes in structural parameters and adsorption energy from ethanethiolate, indicating that there is very small chain length dependency.

### C. Ordered structure

As mentioned in Sec. I, the earlier studies of the structure of alkanethiolates on the gold (111) surface at full coverage reported a hexagonal ( $\sqrt{3}\times\sqrt{3}$ ) $R30^\circ$  structure consisting of molecules densely packed in a single chain model with S-S spacing of  $\sim 5$  Å. The early IR studies show that the hydrocarbon chain should be tilted  $\sim 32^\circ$  if the hexagonal model is assumed. A close inspection of the IR spectra, however, shows a splitting of the methylene modes into two peaks, suggesting two inequivalent chains per unit cell. Fol-

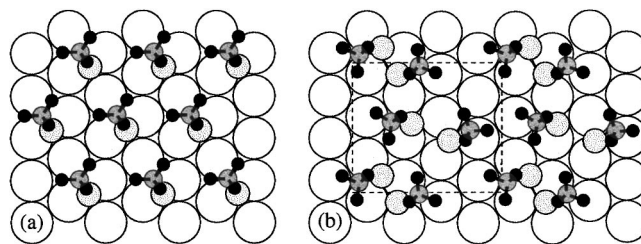


FIG. 10. Showing fully optimized structures, (a) hexagonal and (b)  $c(4\times 2)$  model.

lowing this, LEED, GIXD, and STM studies observed the existence of a  $c(4\times 2)$  superlattice of the hexagonal ( $\sqrt{3}\times\sqrt{3}$ ) $R30^\circ$ . In this model, the unit cell consists of four thiol molecules and two inequivalent chains, which differ in site, height, and rotation ( $\psi$ ). Note that a more conventional notation of  $c(4\times 2)$  is  $(2\sqrt{3}\times 3)$ , but since it was introduced as  $c(4\times 2)$  we proceed to use this notation.

Unfortunately there have been very few quantum mechanical studies of the ordered structure at full coverage. Such a study requires a large number of atoms in the unit cell, and it is therefore extremely CPU intensive to perform structural optimization. However, using the "DACAP" code (massively parallelized over  $k$  points and plane waves) we investigated two proposed structural models for the ordered surface structure of SAM on Au(111) surface at full coverage. Four methylthiolate molecules were adsorbed on a gold (111) surface with  $c(4\times 2)$  symmetry. The slab geometry consists of 72 Au atoms and 13 Å of vacuum. The four thiolate molecules were positioned at different adsorption sites, following experimental suggestions [see Fig. 1(d)], so that only two molecules are distinct [molecules 1 and 2 are equivalent but distinct from 3 and 4, see Fig. 1(d)] with  $d_{S-surf}=2.3$  Å. Based on the experimentally suggested structural configurations, we arranged 12 different models, using two different molecular orientations and a mix of different adsorption sites (top, bri, and hollow) for the molecules.

All structural models then were fully optimized (all atoms in the thiol molecules and the two topmost layers of Au were allowed to relax in all directions and the third Au layer was relaxed in the surface normal direction) until all forces were nearly zero ( $F_{tot}=0.05$  eV/Å). We find that, independent of the starting adsorption site, the thiol molecules relax to one stable structural ordering, where molecules form two dimers distinguished from each other by adsorption site and molecular rotations [the twist angle  $\psi$  and rotation angle  $\phi$ , see Fig. 1(a)]. The adsorption site for sulfur is found to be bri-fcc and bri-fcc for one dimer and bri-top (between bridge and top site) and fcc for the second dimer. The molecular S-C axis, is strongly tilted ( $45^\circ$ – $53^\circ$ ) and hydrogen atoms are twisted with respect to those in the other molecule, Fig. 10. The S-S distances are calculated to 2.34 and 2.46 for the two dimers which are in line with 2.2 Å proposed value by experiment<sup>9</sup> for ordered SAM structure in  $c(4\times 2)$  structure. The energy difference between the hexagonal and  $c(4\times 2)$  model is calculated to be 0.16 eV per  $c(4\times 2)$  unit cell. The calculated structural parameters are summarized in the Table V.

TABLE V. Structural parameters for ordered SAM structure on the Au(111) surface at full coverage. Notations Hex and  $c42$  correspond to the ( $\sqrt{3} \times \sqrt{3}$ ) $R30^\circ$  and  $c(4 \times 2)$  structural models, respectively. Values in the parentheses are for the second dimer.

Property structure model	This work		Ref. 17 $c42$	Expt. 9 $c42$
	Hex	$c42$		
$Z_1, Z_2$ (Å)	2.04	2.78 (2.76), 3.21 (3.14)		$2.21 \pm 0.05, 2.9 \pm 0.05$
$d_{S-Au}$ (Å)	2.50	2.89 (2.85), 3.28 (3.30)		
$d_{S-S}$ (Å)		2.34 (2.46)	$\sim 3.7$	2.20

A comparison between the  $c(4 \times 2)$  structure presented here and the one suggested recently by Vargas *et al.*<sup>17</sup> shows important differences in molecular arrangement. In the Vargas model, the shortest S–S distance has been calculated to be  $\sim 3.7$  Å, with an energy difference of 0.02 eV compared to the hexagonal model. Our analysis of their model, i.e., thiol molecules adsorbed on the bridge site with  $d_{S-S} = 3.7$  Å, shows that the thiol molecules further relax toward the dimmerized state we report.

#### IV. CONCLUSION

One of the important characteristics of SAMs is the presence of multiple energy scales, in contrast to the growth process of simple atomic adsorbates. The formation of an ordered SAM structure depends on several parameters, such as temperature, coverage, chain length, and molecular angle, that contribute to the energetics of the system and therefore play a key role in the growth kinetics. Determination of the energies, including physisorption, chemisorption, chemisorption barrier, corrugation, chain–chain interaction, conformation, and end-group–end-group interaction energy will play a key role in understanding the formation of a SAM structure. While, all these issues are important, the emphasis in this paper have been to understand the structure and energetics of short chain molecules in the initial and final stages.

We have presented a detailed investigation of thiol molecule interactions with the Au(111) surface, using state-of-the-art first-principles calculations. Despite the fact that the van der Waals interaction is not included correctly in our DFT method, we were able to show results that indicate the existence of a physisorbed molecular state, confirming the experimental prediction. The structural properties, including molecular tilt angle and stretched C–C chain, were in accordance with experimental ones. The adsorption of dimethyl disulfide (DMDS) is shown to be coverage dependent. At low coverage, dissociation of DMDS is found to be the dominant reaction. However, at high coverage a stable chemisorbed DMDS was found. The chemisorbed methylthiolate molecules are found to bind at the bridge site slightly shifted toward the fcc site, with the S–C bond tilted from the surface normal toward the bridge site. The driving forces for such behavior are the steric forces and the existence of a preferred Au–S–C angle. The inconsistency in the recent studies regarding the energetic and structural parameters was

also investigated, showing the existence of multiple local minima with respect to the tilting angle, in particular at the fcc site. The effect of coverage and chain length in adsorption energy and structure were also investigated. Finally, the ordered structure of SAM was studied, presenting evidence that the  $c(4 \times 2)$  structure is the preferred one at full coverage, in agreement with all recent experimental results.

Nevertheless, several fundamental issues remain to be investigated, including the growth dynamics of SAMs, interaction of thiol molecules with other metal surfaces, and the differences in the nature of binding in different metals. Theoretical studies of relatively simple thiol molecules interacting with metal surfaces is crucial for future development and application of SAMs.

#### ACKNOWLEDGMENTS

This work was supported by NSF Grant No. DMR 97-02514 and the Air Force Office of Scientific Research, Air Force Materiel Command, USAF, under Grant No. F49620-00-1-0170. A.M.R. would like to thank the Camille and Henry Dreyfus Foundation for support. Computational support was provided by the National Center for Supercomputing Applications, and the ERDC through the high performance computing resources provided by the DoD High Performance Computing Modernization Program and its major shared resource center.

<sup>1</sup>F. Schreiber, *Prog. Surf. Sci.* **65**, 151 (2000).

<sup>2</sup>A. Ulman, *An Introduction to Ultrathin Organic Films* (Academic, Boston, 1991).

<sup>3</sup>A. Ulman, *Chem. Rev.* **96**, 1533 (1996).

<sup>4</sup>S. M. Wetterer, D. J. Lavrich, T. Cummings, S. L. Bernask, and G. Scoles, *J. Phys. Chem. B* **102**, 9266 (1998).

<sup>5</sup>N. Camillone III, P. Eisenberger, T. Y. B. Leung, P. Schwartz, G. Scoles, G. E. Poirier, and M. J. Tarlov, *J. Chem. Phys.* **101**, 11031 (1994).

<sup>6</sup>L. H. Dubois, B. R. Zegarski, and R. G. Nuzzo, *J. Chem. Phys.* **98**, 678 (1993).

<sup>7</sup>N. Camillone, C. E. D. Chidsey, G. Liu, and G. Scoles, *J. Chem. Phys.* **98**, 3503 (1993).

<sup>8</sup>P. Fenter, A. Eberhardt, and P. Eisenberger, *Science* **266**, 1216 (1994); P. Fenter, A. Eberhardt, and K. S. Liang, *Phys. Rev. Lett.* **70**, 2447 (1993).

<sup>9</sup>P. Fenter, F. Schreiber, L. Berman, G. Scoles, P. Eisenberger, and M. J. Bedzyk, *Surf. Sci.* **412/413**, 213 (1998).

<sup>10</sup>G. J. Kluth, C. Carraro, and R. Maboudian, *Phys. Rev. B* **59**, R10449 (1999).

<sup>11</sup>K. M. Beardmore, J. D. Kress, N. Gronbeck-Jensen, and A. R. Bishop, *Chem. Phys. Lett.* **286**, 40 (1998); *Synth. Met.* **84**, 317 (1997).

<sup>12</sup>H. Sellers, A. Ulman, Y. Shnidman, and J. E. Eilers, *J. Am. Chem. Soc.* **115**, 9389 (1993).

<sup>13</sup>H. Grönbeck, A. Curioni, and W. Andreoni, *J. Am. Chem. Soc.* **122**, 3839 (2000).

<sup>14</sup>Y. Yourdshahyan, H. Zhang, and A. M. Rappe, *Phys. Rev. B* **63**, 081405(R) (2001).

<sup>15</sup>T. Hayashi, Y. Morikawa, and H. Nozoye, *J. Chem. Phys.* **114**, 7615 (2001).

<sup>16</sup>Y. Akinaga, T. Nakajima, and K. Hirao, *J. Chem. Phys.* **114**, 8555 (2001).

<sup>17</sup>M. C. Vargas, P. Giannozzi, A. Selloni, and G. Scoles, *J. Chem. Phys.* **105**, 9509 (2001).

<sup>18</sup>D. Krüger, H. Fuchs, R. Rousseau, D. Marx, and M. Parrinello, *J. Chem. Phys.* **115**, 4776 (2001).

<sup>19</sup>J. Gottschalk and B. Hammer, *J. Chem. Phys.* **116**, 784 (2002).

<sup>20</sup>W. Kohn and L. J. Sham, *Phys. Rev.* **140**, A1133 (1965); **145**, A561 (1966).

<sup>21</sup>B. Hammer, L. B. Hansen, and J. N. Nørskov, *Phys. Rev. B* **59**, 7413 (1999).

<sup>22</sup>J. P. Perdew, K. Burke, and M. Ernzerhof, *Phys. Rev. Lett.* **77**, 3865 (1996).



- <sup>23</sup>D. Vanderbilt, Phys. Rev. B **41**, 7892 (1990).
- <sup>24</sup>H. J. Monkhorst and J. D. Pack, Phys. Rev. B **13**, 5188 (1976).
- <sup>25</sup>M. J. Gillan, J. Phys.: Condens. Matter **1**, 689 (1989).
- <sup>26</sup>M. Khein, D. J. Singh, and C. J. Umrigar, Phys. Rev. B **51**, 4105 (1995).
- <sup>27</sup>D. Sutter, H. Dreizler, and H. D. Rudolph, Z. Naturforsch. A **20A**, 1676 (1965).
- <sup>28</sup>J. M. Nicovich, K. D. Kreutter, C. A. van Dijk, and P. H. Wine, J. Phys. Chem. **96**, 2518 (1992).
- <sup>29</sup>D. J. Lavrich, S. M. Wetter, S. L. Bernask, and G. Scoles, J. Phys. Chem. B **102**, 3456 (1998).
- <sup>30</sup>Y. Yourdshahyan, B. Razaznejad, and B. I. Lundquist, Phys. Rev. B **65**, 75416 (2002).